JOURNAL OF SOLID STATE CHEMISTRY **140,** 103–115 (1998)
ARTICLE NO. SC987871

Ab Initio Quantum Mechanical Study of the Structure and Stability of the Alkaline Earth Metal Oxides and Peroxides

Markus Königstein and C. Richard A. Catlow[1]

Davy Faraday Research Laboratory, Royal Institution of Great Britain, 21 Albemarle Street, London W1X 4BS, United Kingdom

Received December 15, 1997; in revised form April 13, 1998; accepted April 14, 1998

We report a detailed computationally study of the stability of the alkaline earth metal peroxides MO_2 (M = Ba, Sr, Ca, Mg, Be) with respect to decomposition into the corresponding oxides MO and molecular oxygen using Hartree–Fock and density functional theory (DFT) techniques. A comparison between calculated and experimental binding energies indicates that the DFT method is most suitable for a correct description of the peroxide bond. The DFT reaction energies for the peroxide decomposition $MO_2 \rightarrow MO + \frac{1}{2}O_2$ show that only BaO_2 and SrO_2 are thermodynamically stable compounds, while CaO_2 (in the calcium carbide structure), MgO_2, and BeO_2 (in the pyrite structure) are energetically unstable with reaction energies of −24.7, −26.8, and −128.7 kJ/mol, respectively, and are therefore unlikely to exist as pure compounds. The published calcium carbide structure for CaO_2 is probably incorrect, at least for pure calcium peroxide, since apart from the thermodynamical instability the compound is more stable in the pyrite structure by 25.5 kJ/mol. Our analysis suggests that the water and/or hydrogen peroxide content of experimentally prepared MgO_2 samples is necessary for the stabilization of the structure, while BeO_2 is clearly unstable under ambient conditions. We studied also the effect of the zero point energies and the entropies on the decomposition free energies and, for this purpose, performed atomistic lattice simulations based on interatomic potentials, which we derived from our *ab initio* data; the results indicate a negligible effect of the zero point energies, while the entropy terms favor the decomposition reaction by ca. 20 kJ/mol at 298.15 K.

1. INTRODUCTION

Of the alkaline earth metal peroxides MO_2 (M = Ba, Sr, Ca, Mg, Be) only BaO_2 and SrO_2 have been prepared in pure form and are well characterized. The main features of the early structural models for these two peroxides proposed by Bernal *et al.* (1) are based on powder diffraction data; they were recently confirmed by single crystal X-ray diffraction (2–4), although the peroxide bond lengths found in the new study are appreciably longer than originally proposed. The crystal structure of these compounds can be considered as a tetragonal distorted rock salt structure, usually referred to as the calcium carbide structure, space group *I*4/*mmm*, where the calcium ions occupy the regular cation positions and the peroxide dumbbells (O_2^{2-}) are centered on the anion positions, while their alignment is along one of the unit cell axes (c axis) of the structure leading to the observed tetragonal distortion, as shown in Fig. 1. Recent single crystal X-ray diffraction investigations (5, 6) on several single crystals of BaO_2 and SrO_2 prepared by high pressure/high temperature experiments established that these two peroxides are nonstoichiometric (MO_{2-x}) with a proportion of the peroxide ions in the crystal structure being replaced by oxide ions. The position of the oxide ions corresponds to the regular positions of the anions in the rock salt structure. The degree of nonstoichiometry varies from near-stoichiometry to compositions corresponding to the replacement of 28% and 10% peroxide by oxide in barium and strontium peroxide, respectively. Furthermore, it was demonstrated (5, 6) that the peroxide bond length varies with the peroxide content in these nonstoichiometric peroxides.

The calcium carbide structure has also been proposed for CaO_2 (7, 8). The structural investigations are based on powder diffraction data of poorly crystalline samples and show additional weak reflections which cannot be attributed to the calcium carbide structure (5, 7), as shown in Fig. 2, indicating that the crystal structure of the compound is uncertain. We note, moreover, that the earlier structures proposed by Kotov *et al.* (7) and Brosset *et al.* (8) have not been confirmed. In addition, calcium peroxide has never been prepared in a pure form: all samples contain water and/or hydrogen peroxide, since the synthetic preparations use water as a solvent and hydrogen peroxide as one of the starting materials (7).

The crystal structure of MgO_2 was reported by Vannerberg (9) on the basis of powder diffraction data: MgO_2, together with the group IIb peroxides ZnO_2 (10) and CdO_2 (11), adopts the pyrite structure illustrated in Fig. 3 (space

---

[1] To whom correspondence should be addressed.

0022-4596/98 $25.00

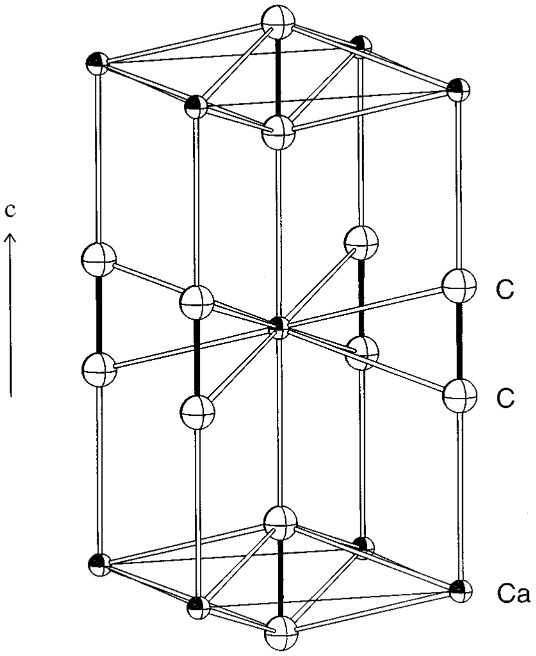

FIG. 1. The calcium carbide structure.

group $Pa\bar{3}$), which can also be derived from that of rock salt, by siting the Mg^{2+} (Zn^{2+} and Cd^{2+}) ions at the cation sites, while the O_2^{2-} groups are again centred around the anion sites and rotated by 45° from the direction of the cubic axes. As for the case of CaO_2, it has not proved possible to prepare MgO_2 in a pure form, with all samples again containing water and/or hydrogen peroxide from the preparation procedure (9, 12). Moreover, the question of whether water and/or hydrogen peroxide is included as part of the crystal structure or only physically adsorbed is not easy to decide partly because only powder data are available for this material (13). It is also uncertain as to whether the presence of water and/or hydrogen peroxide is essential for the stabilization of the crystal structure of MgO_2 or whether it should be possible in principle to prepare the pure material.

Budnikov *et al.* (14) suggested that BeO_2 might be present in the products of the action of hydrogen peroxide on freshly precipitated hydroxide or basic carbonates following previous doubtful reports of the compound (15). The preparation of the peroxide by the action of ozone on beryllium hydroxide suspended in Freon 12 at $-65°C$ was claimed by Vol'nov *et al.* (16) but without giving further characterisation of the compound. However, Wriedt (17) remarks that BeO_2 is unstable and it is questionable whether it has been prepared at all. The comprehensive review by Vannerberg (18) also failed to find any report of the formation of BeO_2.

In view of the many uncertainties in the experimental data regarding these systems, we report in this paper a detailed survey of their structures and energetics using computer simulation methods. In contrast to the alkaline earth metal oxides, there are no previous *ab initio* calculations reported for the alkaline earth metal peroxides. We report in two separate publications (19, 20) details of the electronic structure of the stoichiometric alkaline earth metal peroxides BaO_2, SrO_2, and CaO_2 and of the structure and thermodynamic stability of the nonstoichiometric peroxides BaO_{2-x} and SrO_{2-x}; here we focus on the thermodynamical stability of the stoichiometric alkaline earth metal peroxides MO_2 (M = Ba, Sr, Ca, Mg, Be) with respect to decomposition to the corresponding oxides and molecular oxygen. In order to gain reliable evidence concerning the stability of the peroxides, we will use two different types of arguments: first we use structural considerations, which are based on the assumption that, in similar ionic structures, the bond lengths should be comparable. Since, as we have seen, the calcium carbide and the pyrite structures of the peroxides can easily be derived from the rock salt structure adopted by the alkaline earth metal oxides (BeO is an exception as it crystallizes in the wurtzite structure), we have as a good criterion for the stability of the peroxides that the metal–oxygen bond lengths for the oxides and the corresponding peroxides are similar. Secondly, we investigate directly the thermodynamic stability of the peroxides by calculating internal energies and Gibbs free energies of the peroxide decomposition reaction, where the peroxides decompose to the corresponding oxides and molecular oxygen.

Our paper is organized as follows: after some brief methodological considerations in Section 2, we discuss in Section 3 the results of our calculations. In Section 3.1 we comment first on the optimised geometries and draw, from structural considerations, preliminary conclusions as to the stability of the alkaline earth metal peroxides. Secondly, we discuss, in Section 3.2, the energetics of the peroxide decomposition reaction $MO_2 \rightarrow MO + \frac{1}{2}O_2$. In order to gain an estimate of the accuracy of our calculated energies, we consider first the comparison between calculated and experimental binding energies of the peroxides, oxides and the oxygen molecule. Afterwards, we report *ab initio* decomposition energies and finally we estimate the influence of the zero point energies and entropies on the reaction energetics. In Section 4, we draw our conclusions regarding the structure and stability of the alkaline earth metal peroxides on the basis of all the results obtained in this study and our related work in Ref. (19).

2. METHODOLOGY

Our calculations employed the *ab initio* techniques available in the CRYSTAL95 code (21) which uses the periodic self-consistent field approach, where the Bloch functions are expanded in localised basis sets of atomic orbitals; their

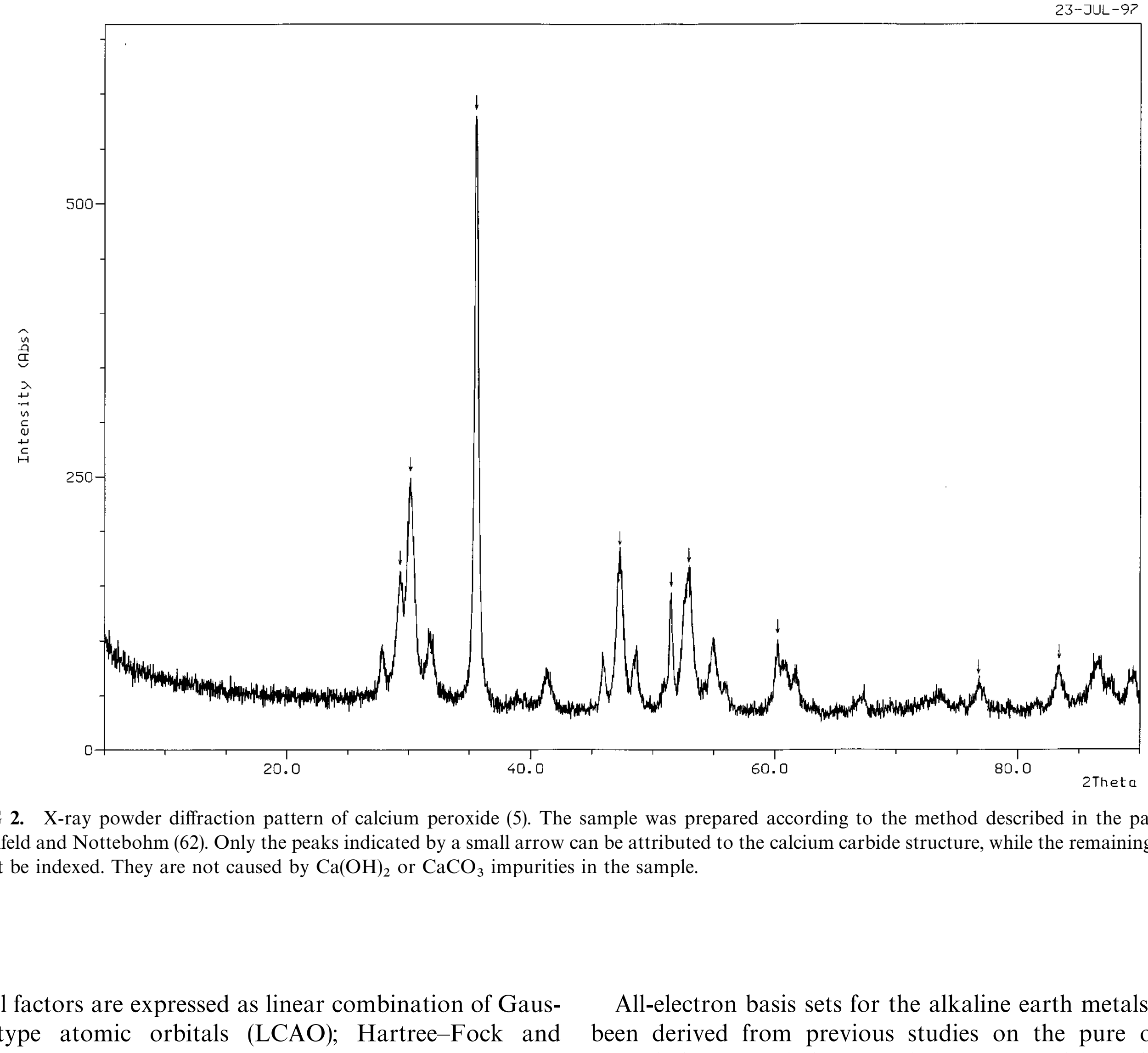

FIG 2. X-ray powder diffraction pattern of calcium peroxide (5). The sample was prepared according to the method described in the paper by Riesenfeld and Nottebohm (62). Only the peaks indicated by a small arrow can be attributed to the calcium carbide structure, while the remaining peaks cannot be indexed. They are not caused by $Ca(OH)_2$ or $CaCO_3$ impurities in the sample.

radial factors are expressed as linear combination of Gaussian-type atomic orbitals (LCAO); Hartree–Fock and Kohn–Sham Hamiltonians are available.

In our work we used both the Hartree–Fock (HF) and density functional theory (DFT) methods. The HF results have been corrected by estimates of the effects of electron correlation: having calculated the HF energy and wave function, the correlation correction to the energy is evaluated *a posteriori* with a density functional of the Hartree–Fock equilibrium density, according to the generalized gradient approximation (GGA) scheme, Perdew 91 (22, 23), which was derived from density functional theory. Causà *et al.* (24, 25) have described in detail this integration of *a posteriori* functionals on the electronic density obtained with the Hartree–Fock method and also the recent implementation of the DFT method in the periodical LCAO environment of the CRYSTAL95 code. Density functional calculations are performed in the nonlocal density approximation using the Perdew–Wang, PW91, gradient corrected exchange and correlation functionals (22, 26).

All-electron basis sets for the alkaline earth metals have been derived from previous studies on the pure oxides BeO (27), MgO (28), CaO (29). Hay–Wadt, small-core pseudopotentials were used for strontium and barium as previously derived for SrO (30) and reported elsewhere for BaO (19). The all-electron basis set for oxygen was taken from Ref. (31) using the exponents of 0.500, 0.149, and 1.000 bohr^{-2} for the $3sp$ and $4sp$ and the $3d$ shells, respectively.

As regards the computational conditions, high numerical accuracy is required to study the stability of the peroxides with respect to the oxides and molecular oxygen. Therefore the following values have been used for the truncation tolerances in the evaluation of the Coulomb and exchange series (21, 32): 6, 8, 6, 7, 14. The reciprocal space integration was performed by sampling the first Brillouin zone at a regular array of $8 \times 8 \times 8$ k points. At this level of accuracy, numerical errors are reduced to a minimum. Further details of our quantum mechanical calculations are given elsewhere (19).

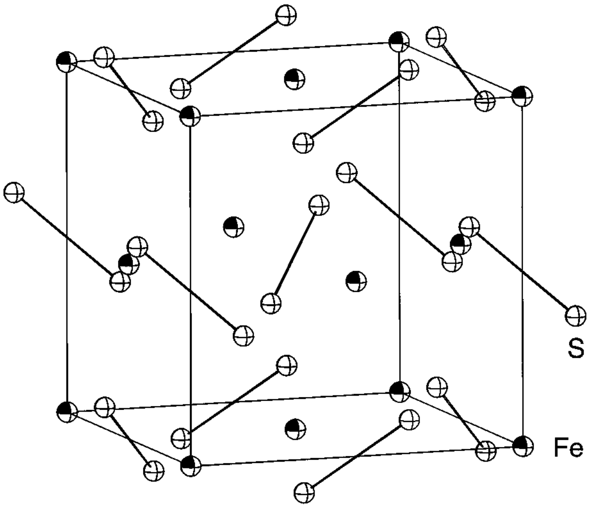

FIG 3. The pyrite structure.

In order to study the effect of the zero point energies and the entropies on the decomposition energetics, we additionally performed atomistic lattice simulations using interatomic potentials, employing the computer code GULP (33, 34). After minimizing the energy of a structure with respect to all unit cell parameters and internal degrees of freedom, this code calculates, for the optimized structure, second derivatives of the energy with respect to both internal and external strains. From the resulting dynamical matrix, vibrational frequencies may be calculated, from which the phonon density of states can be obtained. From the latter, we may calculate a wide range of quantities, including the zero point energy and the entropy at a specified temperature. More details of the techniques employed in the static lattice simulations are given in Ref. (35), while a detailed discussion of the theory of lattice dynamics is presented in Ref. (36).

3. RESULTS AND DISCUSSION

3.1. Optimized Geometries and Structural Considerations

(a) Optimized geometries. We first consider the optimized structures of the alkaline earth metal peroxides, oxides, and the oxygen molecule; the results for latter are needed to construct appropriate thermodynamical cycles. For BeO_2 we assumed the same crystal structure as for MgO_2, i.e. the pyrite structure, and for CaO_2 we performed calculations on the calcium carbide as well as the latter structure. DFT techniques were used for all structures, while for the calcium carbide structure we also employed the Hartree–Fock (HF) method and the Hartree–Fock method with *a posteriori* correction of the electron correlation (HF + corr). In Table 1, we report the optimized structural parameters for BaO_2, SrO_2, and CaO_2 in the calcium carbide structure and

TABLE 1

Calculated and Experimental[a] Structural Parameters for the Peroxides (Calcium Carbide Structure) and Oxides (Rock Salt Structure) of Barium, Strontium, and Calcium: The Equilibrium Lattice Parameter(s) a_0 (and c_0), Unit Cell Volume V_0, Oxygen Fractional Coordinate z(O), Peroxide Bond Length $d_{O\text{-}O}$, Zero Pressure Bulk Modulus B_0, and Its Pressure Derivative B' are Reported for Calculations Involving Hartree–Fock, Hartree–Fock and *a Posteriori* Corrections for Electron Correlation (HF+corr) and DFT Methods

	Hartree–Fock			HF + corr			DFT			Experiment		
MO_2	BaO_2	SrO_2	CaO_2	BaO_2	SrO_2	CaO_2	BaO_2	SrO_2	CaO_2	BaO_2	SrO_2	CaO_2
a_0 [Å]	3.92	3.65	3.40	3.79	3.54	3.29	3.84	3.58	3.29	3.806	3.563	(3.54)
c_0 [Å]	7.00	6.69	6.56	6.69	6.39	6.20	6.93	6.70	6.65	6.837	6.616	(5.92)
V_0 [$Å^3$]	107.59	89.17	76.00	95.88	79.86	66.96	102.31	85.89	72.17	99.03	83.99	(74.2)
z(O)	0.3964	0.3916	0.3895	0.3954	0.3905	0.3871	0.3896	0.3858	0.3850	0.3908	0.3879	(0.39)
$d_{O\text{-}O}$ [Å]	1.45	1.45	1.45	1.40	1.40	1.40	1.53	1.53	1.53	1.493	1.483	(1.30)
B_0 [GPa]	74.5	84.9	—	95.6	112.6	143.0	72.3	90.4	107.5	64.0	—	—
B'	4.03	4.67	—	4.26	5.16	4.08	5.91	4.38	3.86	(4.00)	—	—
MO	BaO	SrO	CaO	BaO	SrO	CaO	BaO	SrO	CaO	BaO	SrO	CaO
a_0 [Å]	5.617	5.191	4.847	5.435	5.050	4.708	5.552	5.132	4.797	5.539	5.160	4.811
B_0 [GPa]	83.4	114.7	127.0	103.5	138.2	150.0	81.5	117.9	124.7	82.5	96.5	116.3
B'	4.48	5.13	4.12	4.23	4.82	6.49	4.71	4.19	4.14	5.37	5.08	4.79

[a] The experimental crystallographic data for BaO_2 and SrO_2 are from Ref. (5), for CaO_2 from Ref. (7), and for the oxides from Ref. (57). The bulk modulus for BaO_2 is obtained from the p–V data reported in Ref. (5) ($p < 5$ GPa, $T = 298$ K) by fitting them using the Vinet equation of state (58, 59); the experimental data are insufficiently accurate to fit a reasonable value of B', which is therefore fixed at 4.00, which is justified by comparison with similar materials. The bulk moduli for the oxides, which are linearly extrapolated to 0 K, and their derivatives are from Ref. (60).

TABLE 2

Calculated (DFT Method) and Experimental[a] Structural Parameters for CaO_2, MgO_2, and BeO_2 in the Pyrite Structure, for CaO and MgO in the Rock Salt Structure and BeO in the Wurtzite Structure: The Lattice Parameter(s) a_0 (and c_0), Oxygen Fractional Coordinate x(O) [or z(O)], Peroxide Bond Length $d_{O\text{–}O}$, Zero Pressure Bulk Modulus B_0, and Its Pressure Derivative B' are Reported

	DFT			Experiment	
MO_2	CaO_2	MgO_2	BeO_2	MgO_2	BeO_2
a_0 [Å]	5.45	4.91	4.30	4.839	—
x(O)	0.0800	0.0882	0.0994	0.0890	—
$d_{O\text{–}O}$ [Å]	1.51	1.50	1.48	1.492	—
B_0 [GPa]	99.4	132.7	224.0	—	—
B'	4.21	3.15	4.01	—	—
MO	CaO	MgO	BeO	MgO	BeO
a_0 [Å]	4.797	4.260	2.70	4.213	2.698
c_0 [Å]	—	—	4.36	—	4.380
z(O)	—	—	0.379	—	0.378
B_0 [GPa]	124.7	154.1	225.6	162.3	224.4
B'	4.14	4.24	3.96	4.22	—

[a] The experimental crystallographic data for MgO_2 are from Ref. (9) and for the oxides from Ref. (57). The bulk modulus and its derivative for MgO is from Ref. (61), and for BeO from Ref. (44).

for the corresponding oxides (for which HF, HF + corr, and DFT methods were used); Table 2 contains the structural parameters for CaO_2, MgO_2, and BeO_2 in the pyrite structure and for the corresponding oxides (based only on the DFT method). The calculations of the alkaline earth metal oxides were undertaken in the experimentally observed rock salt structure, except for BeO which crystallizes in the wurtzite structure (hexagonal close-packed structure; space group $P6_3mc$).

On comparing the lattice constants of the optimized structures, using the HF, HF + corr, and DFT method, we observe the same behaviour as found in previous publications [see e.g. Refs. (37, 38)]: the HF and DFT method, which use GGA correlation and exchange functionals, usually overestimate lattice constants, but the error is larger in the HF than in the DFT calculations; on the other hand, the HF + corr method underestimates in general the lattice constants with respect to the HF values and also with respect to the experimental values. The approximate character of the *a posteriori* correlation correction in the latter results in an inaccurate estimate of the correlation contribution to the first and second derivatives of the energy with respect to the volume: the bulk moduli are therefore usually significantly overestimated. In particular, we find for the oxides BaO, SrO, and CaO, that the HF method overestimates the lattice constants, on average by 0.9%, with respect to the experimental lattice constants, while the HF + corr method underestimates them by 2.0% and the DFT values are close to the experimental values (Table 1). The same behavior is found for the peroxides BaO_2 and SrO_2: the average deviation of the a and c lattice parameters for the HF, HF + corr, and DFT values from the experimental values is + 2.2, − 1.7, and + 1.0%, respectively, and the bulk moduli are considerably higher in the HF + corr calculations as compared to the HF or DFT values. Results for CaO_2 are discussed later.

We now turn our attention to the covalent peroxide bond. It is well known from molecular calculations that the DFT method, which uses GGA correlation and exchange functionals, overestimates covalent bonds lengths [see e.g. Refs. (39, 40), which is also observed in our study: for BaO_2 the peroxide bond length is overestimated by 2.5% by the DFT method, while we find that the HF method underestimates this bond length, in contrast to the lattice parameters, by 2.9%; the HF + corr method underestimates this quantity by 6.2%. The same trend can be observed for the optimized bond lengths in the oxygen molecule (which are not reported in the tables): the HF, HF + corr, and DFT method give values of 1.17, 1.15, and 1.23 Å compared to the experimental value of 1.207 Å (41).

Considering our results for CaO_2, we note first that the calculated c lattice parameter is considerably larger with respect to the experimental value reported by Kotov (7) in 1941, while the a lattice parameter is considerably smaller: e.g. the DFT calculations which give, as we have seen, the most accurate description of the cell parameters, predict values that differ by − 7.0% (a lattice parameter) and + 12.3% (c lattice parameter) from the experimental data. We note that none of the other crystal structures studied here with the DFT method had errors which were larger than + 1.3%. We emphasize furthermore, as already commented in the Introduction, that the experimental data were obtained using powder diffraction techniques on poorly crystalline samples. The powder diffraction pattern contained additional reflections which could not be attributed to the tetragonal unit cell (5, 7). In the light of our calculations and the uncertainties surrounding the experimental data, it appears likely that CaO_2 may crystallize in a different structure or may even be unstable in a pure form. The next section considers its structure in detail.

We note, finally, that the features which we found for the DFT method, namely, the relatively close agreement of experimental and calculated lattice parameters and the overestimation of the peroxide bond lengths, are of course also valid for the peroxides in the pyrite structure and for the corresponding oxides of calcium, magnesium, and beryllium, as is evident from Table 2.

(b) Structural considerations. After having optimized the geometry of the oxides, peroxides, and the oxygen molecule,

we can now analyze the calculated (and also experimental) structures in more detail and from our analysis of the metal–oxygen bond lengths we are able to comment on the stability of the different alkaline earth metal peroxides. Our structural considerations are based on the general observation that in stable ionic materials, bond lengths of a given type are usually comparable. Therefore, a peroxide structure is very likely to be unstable if the metal–oxygen bond lengths differ considerably from the metal–oxygen bond lengths in the corresponding oxide. We also use the less widely employed argument of bond compressibilities. We would generally expect, for a stable crystal structure, that the bond compressibilities for individual bonds decrease when we move from the oxides or peroxides of the heavier to those of the lighter alkaline earth metal oxides or peroxides with the same crystal structure. Furthermore, we expect that, for stable peroxides, the metal–oxygen bond compressibilities are higher than in the corresponding oxides, since the peroxides are less dense than the close-packed oxides.

We first consider barium and strontium peroxide in the calcium carbide structure and the corresponding oxides (Table 3[A]). We examine only the values obtained from our DFT calculations. We note that the metal ions in the peroxides with the calcium carbide structure are surrounded by ten oxygen ions with two different metal–oxygen bond lengths, as is evident from Fig. 1, where we see two equivalent bonds pointing along the *c* direction and eight other (equivalent) bonds. In order to compare the metal–oxygen bond lengths of the peroxides more easily with those of the oxides, we also report in Table 3[A] the average metal–oxygen bond lengths for the peroxides in the calcium carbide structure. We find, in general, very good agreement between calculated and experimental metal–oxygen bond lengths in both the oxides and peroxides: the errors are usually less than 1%. Furthermore, we find that the average metal–oxygen bond length in the peroxide is always either nearly the same (as in BaO_2) or slightly longer (as in SrO_2) than the corresponding quantity in the oxides. The two metal–oxygen bonds of the peroxide, pointing along the crystallographic *c* axis [*M*–O (2 ×)], are smaller for BaO_2 by about 0.1 Å than the metal–oxygen bond in BaO, while for SrO_2 these two bond lengths are nearly equal. We note that, as we have shown elsewhere (19), our calculations yield a compressibility of the metal–oxygen bonds pointing along the crystallographic *c* axis which is 62% higher for BaO_2 than for SrO_2. We emphasize that the peroxide bond which also points along the *c* axis is, on the other hand, rigid, i.e. it shows, in all the peroxides investigated, only a negligible compressibility compared to the compressibility of the metal–oxygen bonds. The remaining eight metal–oxygen bonds [*M*–O (8 ×)] are up to 0.08 Å (3%) longer in BaO_2 and SrO_2 than in BaO and SrO.

TABLE 3
Calculated (DFT Method) and Experimental (Exp.) Metal–Oxygen Bond Lengths [Å] for the Peroxides and Oxides[a]

		Barium		Strontium		Calcium	
[A]	Bond	DFT	Exp.	DFT	Exp.	DFT	Exp.
MO_2	*M*–O (2 ×)	2.700	2.672	2.585	2.566	2.560	2.23[b]
	M–O (8 ×)	2.823	2.793	2.645	2.626	2.452	2.61[b]
	M–O (∅)	2.798	2.769	2.633	2.614	2.474	2.53[b]
MO	*M*–O (6 ×)	2.776	2.770	2.566	2.580	2.399	2.406

		Calcium	Magnesium		Beryllium	
[B]	Bond	DFT	DFT	Exp.	DFT	Exp.
MO_2	*M*–O (6×)	2.371	2.113	2.08	1.826	—
MO	*M*–O (6×)	2.399	2.130	2.107	1.647 (3 ×) 1.652 (1×)	1.647 (3×) 1.656 (1×)

[a] The references for the experimental data are given in Tables 1 and 2. *M*–O (∅) indicates the average *M*–O bond length in the peroxides. [A] Peroxides in the calcium carbide structure; [B] Peroxides in the pyrite structure.

[b] It is assumed that the O–O bond length is 1.47 Å. (The values for peroxide bond lengths were too short in older publications: compare e.g. Ref. (1) and (5) for BaO_2 and SrO_2.)

For CaO_2, in the calcium carbide structure, we have a completely different picture: while the calculated *M*–O (8 ×) bonds are longer than in CaO, as we also found for BaO_2 and SrO_2, the calculated *M*–O (2 ×) bonds are, in contrast to BaO_2 and SrO_2, considerably longer (7%) than in CaO and also clearly longer than the *M*–O (8 ×) bonds, indicating the instability of the structure. The instability is also confirmed by the *M*–O (2 ×) bond compressibility from CaO_2 which is higher in CaO_2 than in SrO_2, as discussed in Ref. (19). We note, furthermore, that the calculated two metal–oxygen bonds of the peroxide pointing along the crystallographic *c* axis [*M*–O (2 ×)] are nearly equal in CaO_2 and in SrO_2 (as is, of course, the case for the calculated *c* lattice parameter of CaO_2 and SrO_2, as shown in Table 1), from which it is clear that we have anion–anion contacts in the proposed calcium carbide structure of CaO_2 and therefore a strong repulsive force in the *c* direction between the peroxide ions leading to the instability of the crystal structure. This is also confirmed by charge density plots which show that the density between the two peroxide groups pointing along the *c* axis of the unit cell is higher in CaO_2 (0.015 au) than in SrO_2 (0.010 au) and BaO_2 (0.010 au).

We now consider the experimental bond lengths for CaO_2. The experimental *M*–O (2 ×) bonds are smaller than those in CaO by 0.18 Å, which suggests that the calcium-oxygen bond lengths are questionable in the peroxide: the *M*–O (8 ×) bonds are on the other hand considerably longer (8%) than in CaO, leading to differences between the *M*–O

(2 ×) and M–O (8 ×) bonds, in the same crystal structure, of 0.38 Å which are unrealistically high. It is also worth mentioning that Vannerberg (18) concluded, from ionic radii considerations, that there must be anion–anion contacts in the experimentally proposed crystal structure of CaO_2. This analysis underlines the uncertainties in the reported CaO_2 structure.

We turn now to the peroxides with the pyrite structure reported in Table 3[B]. We find that for CaO_2 and MgO_2, the metal–oxygen bond lengths are nearly the same in the peroxides and oxides, which indicates, especially for CaO_2, that the pyrite structure is probably more stable than the calcium carbide structure. In contrast we find for BeO_2 that the metal–oxygen bond lengths are considerably longer (0.18 Å or 11%) than in BeO showing that BeO_2 is obviously unstable in the pyrite structure, a point which we confirm later when we discuss the energetics of the peroxides. We also note that the same conclusion concerning the instability of BeO_2 in the pyrite structure can be obtained from ionic radii considerations. In particular Vannerberg (18) has shown that the ionic radius of beryllium is too small for the compound to be stable with the pyrite structure.

In order to complete the picture of the peroxides in the pyrite structure, we report, in Table 4, the calculated bond compressibilities for CaO_2, MgO_2, and BeO_2 and for the corresponding oxides, following the similar analysis for the peroxides BaO_2, SrO_2, and CaO_2 in the calcium carbide structure given in Ref. (19). We note, first, that the bond and cell edge compressibility decrease, as we would expect, in the order $CaO_2 > MgO_2 > BeO_2$. But secondly, we find that the calculated metal–oxygen bond compressibility in BeO is by 14% longer than the corresponding quantity in the peroxide (the two slightly different M–O bonds in the wurtzite structured BeO show nearly the same bond compressibility). This behavior contrasts with that of the other two oxides, where their bond compressibility is always smaller than in the peroxides and once more demonstrates the instability of BeO_2.

TABLE 4

Coefficients D_1 and D_2 of the Parabolic Approximation $r/r_0 = 1 - D_1 p + D_2 p^2$, Fitted Using the Least-Squares Method for the Pressure Dependence of the Lattice Constants and Bond Lengths (DFT Calculations)[a]

	Calcium		Magnesium		Beryllium	
Compound	D_1 (TPa^{-1})	D_2 (TPa^{-2})	D_1 (TPa^{-1})	D_2 (TPa^{-2})	D_1 (TPa^{-1})	D_2 (TPa^{-2})
MO_2						
a/a_0	3.14	28	2.40	17	1.13	3
d_{O-O}/d^0_{O-O}	1.54	14	0.82	0	0.68	1
d_{M-O}/d^0_{M-O}	3.33	30	2.55	19	1.18	3
MO						
d_{M-O}/d^0_{M-O}	2.33	15	1.82	9	1.34	5

[a] Values are reported for the peroxides (pyrite structure) and oxides of calcium, magnesium, and beryllium. The coefficient D_1 is equal to the first-order bond or cell edge compressibility.

3.2. *Energetics of the Peroxide Decomposition*

(a) Binding energies. In order to estimate the accuracy of the calculated energies with the HF, HF +corr, and DFT methods, we report in this section first the binding energies of the oxides, the peroxides, and the oxygen molecule obtained with the different methods and compare these values with experimental data. In the next section, we report decomposition energies in order to gain evidence concerning the stability of the different peroxides.

The binding energies at 0 K under static conditions were calculated as the differences between the total crystal energies per formula unit (or the energy of the isolated oxygen molecule) and the energies of the constituent isolated atoms. The HF, HF +corr, and DFT binding energies are reported in Table 5, together with the experimental values and the calculated total energies for individual atoms, the peroxides, the oxides, and the oxygen molecule. Atomic energies and the energy of the oxygen molecule were obtained from the calculations using the same basis set as for the crystal calculations, but supplemented by two additional diffuse shells, the exponents of which were optimized. The corresponding experimental values of the binding energies [E^0_B(exp.)] were derived by appropriate Born–Haber thermochemical cycles of the type

$$E^0_B(\text{exp.}) = \Delta H_f^{298} - (H^{298} - H^0) - E^0_{\text{vib}} - \sum_i [\Delta H^{298}_{a,i} - (H_i^{298} - H_i^0)].$$

The sum is extended to all chemical elements in the formula unit. All values involved are reported in Table 6. Formation enthalpies ΔH_f^{298} of the oxides, sublimation (M), and dissociation (O_2) enthalpies ΔH_a^{298} and the enthalpy changes $H^{298} - H^0$ for all chemical species involved were taken from Ref. (42). The zero point vibrational energies E^0_{vib} of all oxides were estimated using the Debye model; the Debye temperatures of 232, 401, 605, 945, and 1280 K for BaO, SrO, CaO, MgO, and BeO, respectively, are from Refs. (43) and (44); E^0_{vib} of the oxygen molecule was calculated using the *ab initio* quantum chemistry package DMOL[2] (45), the methodology of which was described by Delley (46). In the

---

[2] The basis set for the spin-polarized optimization was a DNP (double-numerical plus polarization). The calculations were performed using a fine integration grid and the functionals BP (Perdew–Wang 1991 correlation functional and Becke's 1988 version of a gradient corrected exchange functional).

TABLE 5

Total Energies per Formula Unit (Hartree) and Binding Energies (kJ/mol) for Individual Atoms, the Peroxides, Oxides, and the Oxygen Molecule[a]

	Total energies (Hartree)			Binding energies (kJ/mol)			
	HF	HF + corr	DFT	HF	HF + corr	DFT	Experiment
E(O)	− 74.8089	− 75.0625	− 75.0540				
E(Ba)	− 24.8957	− 25.2058	− 25.2244				
E(Sr)	− 30.0966	− 30.4236	− 30.4223				
E(Ca)	− 676.7239	− 677.5677	− 677.5280				
E(Mg)	− 199.6046	− 200.0520	− 200.0428				
E(Be)	− 14.5635	− 14.6580	− 14.6372				
E(BaO)	− 99.9277	− 100.5904	− 100.6507	− 586.0	− 845.6	− 977.7	− 974.8
$E(BaO_2)$	− 174.7763	− 175.7408	− 175.8393	− 689.9	− 1076.7	− 1330.8	− 1308.2
E(SrO)	− 105.1421	− 105.8175	− 105.8342	− 620.9	− 870.0	− 939.6	− 1006.3
$E(SrO_2)$	− 179.9770	− 180.9538	− 181.0162	− 689.2	− 1063.8	− 1275.7	− 1305.6
E(CaO)	− 751.8061	− 752.9980	− 752.9902	− 717.5	− 965.6	− 1071.7	− 1067.5
$E(CaO_2)$	− 826.6135	− 828.1077	− 828.1473	− 713.3	− 1089.8	− 1342.3	(− 1336.3)
$E^{\text{pyrite}}(CaO_2)$			− 828.1570			− 1367.8	
E(MgO)	− 274.6766	− 275.4690	− 275.4677	− 690.7	− 930.7	− 973.7	− 1008.9
$E^{\text{pyrite}}(MgO_2)$			− 350.6239			− 1242.1	(− 1268.0)
E(BeO)			− 90.1491			− 1202.2	− 1200.6
$E^{\text{pyrite}}(BeO_2)$			− 165.2665			− 1368.6	
$\frac{1}{2}E(O_2)$	− 74.8348	− 75.1213	− 75.1665	− 67.7	− 154.4	− 295.4	− 251.2

[a] Hartree–Fock (HF), *a posteriori* for electron correlation corrected Hartree–Fock (HF + corr), DFT and experimental values are reported. The energies for the peroxides BaO_2, SrO_2, and CaO_2 refer to the calcium carbide structure; additionally we report for CaO_2, MgO_2, and BeO_2 DFT energy values in the pyrite structure. The experimental values are obtained from thermodynamical cycles with the data of Table 6.

case of the peroxides, Debye temperatures or elastic constants to derive the zero point energies and heating enthalpies are not available and the binding energies were therefore calculated only from the formation enthalpies ΔH_f^{298} of the peroxides (18, 47) and the sublimation (M) and dissociation (O_2) enthalpies ΔH_a^{298}. We emphasize that the experimental formation enthalpies for CaO_2 and MgO_2 are unreliable, since they cannot be prepared experimentally without a significant water and/or hydrogen peroxide content as commented in the Introduction. The experimental binding energies for CaO_2 and MgO_2 are therefore placed in brackets in Table 5.

The Hartree–Fock binding energies are, as expected, very much underestimated with respect to the experimental values (31), i.e. by 32–40% for the oxides and by 47% for the peroxides. Consequently the Hartree–Fock results are of little use in calculating the decomposition energies. The error, due to the neglect of the electron correlation contribution to the energies, can be corrected substantially using an *a posteriori* estimate based on density functional theory (22, 23): the absolute values of the HF + corr binding energies are now lower than the experimental values by ca. 80–140 kJ/mol (8–14%) for the oxides and by 240 kJ/mol (18%) for the peroxides. On the other hand, it is striking

TABLE 6

Formation (ΔH_f^{298}), Sublimation or Dissociation (ΔH_a^{2298}) and Heating ($H^{298}-H^0$) Enthalpies and Zero Point Vibrational Energies (E_{vib}^0) Used in the Thermodynamical Cycles Yielding the Experimental Binding Energies (See Text for References) (Units are in kJ/mol)

	Ba	Sr	Ca	Mg	Be	O	BaO	SrO	CaO	MgO	BeO	O_2
ΔH_f^{298}							− 548.0	− 592.0	− 634.9	− 601.6	− 609.4	0.0
ΔH_a^{298}	180.0	164.4	177.8	147.1	324.0	249.2						
E_{vib}^0							4.34	7.50	11.3	17.7	23.9	9.020
$H^{298} - H^0$			5.736	4.998	1.950	6.725			6.75	5.160	2.837	8.680

that the absolute error for the peroxides BaO_2 and SrO_2 is nearly twice as large as for the oxides; the difference of the errors in the binding energies of BaO_2 and SrO_2 with respect to BaO and SrO is 105 kJ/mol. It follows that electron correlation is more important in peroxides than in oxides and self consistent (not *a posteriori*) calculation of the electron correlation energies via the DFT method is therefore desirable for a good description of the energetics of the peroxides. The binding energies of both the oxides and the peroxides calculated with the DFT method are in very good agreement with experimental values with the deviations from experiment being only in the range of 0 and 3%, with the exception of SrO, the binding energy of which is underestimated by 6.6%. However, we note that we have now a small overestimation of the binding energies of BaO_2 and SrO_2 compared with that of BaO and SrO of ca. 20 and 37 kJ/mol.

We turn now to the binding energies of the oxygen molecule. It is well known that the binding energies calculated for diatomic molecules are not satisfactory using the Hartree–Fock method (48, 49), which underestimates the binding energy of the oxygen molecule by more than 70% and the underestimation remains still approximately 40% when the correlation energy is included by an *a posteriori* calculation; on the other hand the DFT method overestimates this energy value by 18%. This has two important consequences: first, the underestimation of the binding energy of the oxygen molecule in the HF +corr method is approximately cancelled by the underestimation of the binding energy of BaO_2 relative to BaO or SrO_2 relative to SrO. Secondly, the overestimation of the binding energy in the oxygen molecule with the DFT method is similarly partially cancelled in the calculation of decomposition energies by the overestimation of the binding energies of the peroxides relative to the oxides.

We have seen that correlation plays an important role in the peroxides and its inclusion is more important in the peroxides than in the oxides. Both the HF +corr and DFT method lead to large errors in the binding energies of the oxygen molecule, but these errors cancel at least partially the errors in the binding energies of the peroxides with respect to the corresponding oxides. Therefore it is, in principle, possible to use the HF +corr and the DFT method for the calculation of the peroxide decomposition energies and we will see in the next section that both methods give indeed similar energies for these reaction. Since, however, the absolute and relative errors of the binding energies are considerably smaller in the DFT method than in the HF +corr method, we consider the former to be most reliable for the calculation of binding energies and therefore also for the calculation of reliable decomposition energies and will use it exclusively for the peroxides in the pyrite structure.

(b) Ab initio decomposition energies. We now investigate directly the thermodynamic stability of the peroxides. The energies of the decomposition reaction ΔE_R^0 of the peroxides $MO_2 \rightarrow MO + \frac{1}{2}O_2$ at zero pressure and 0 K in static conditions were computed as differences between the total crystal energies per formula unit of the oxide and the peroxide plus half of the energy of the isolated oxygen molecule. The thermodynamic stability of a peroxide at 0 K is indicated by a positive reaction energy, while a negative ΔE_R^0 indicates instability. We stress that the calculation of these reaction energies is challenging, since their absolute values are smaller than the values of the binding energies by a factor of usually more than 20, and therefore even the small errors in the binding energies of the oxides and peroxides can cause large errors in the reaction energies. The Hartree–Fock, Hartree–Fock plus *a posteriori* correlation correction, and DFT decomposition reaction energies are reported in Table 7 together with the available experimental values (50–52) for BaO_2, SrO_2, and CaO_2. (We note again that CaO_2 cannot be prepared experimentally without a significant water and/or hydrogen peroxide content. The experimental decomposition energies are therefore unreliable and placed in brackets in Table 7.)

We consider, first, the decomposition energies of BaO_2, SrO_2, and CaO_2 in the calcium carbide structure and later the same quantities for CaO_2, MgO_2, and BeO_2 in the pyrite structure. Both the HF +corr and the DFT calculations predict correctly that BaO_2 and SrO_2 are thermodynamically stable compounds. For SrO_2, the decomposition energies agree very well with the experimental values of Vedeneev *et al.* (51), while for BaO_2 the HF +corr values are also in very good agreement with experiment (50–52) but

TABLE 7
Reaction Energies $\Delta E_R(MO_2)$ for the Reaction $MO_2 \rightarrow MO + \frac{1}{2}O_2$[a]

				Experiment		
	HF	HF +corr	DFT	Ref. (50)	Ref. (51)	Ref. (52)
$\Delta E_R(BaO_2)$	36.2	76.4	58.0	75.6	76.2	75.0
$\Delta E_R(SrO_2)$	0.3	39.4	40.7	53.4	40.2	50.5
$\Delta E_R(CaO_2)$	− 71.9	− 30.5	− 24.7	(16.0)	(15.1)	
$\Delta E_R^{pyrite}(CaO_2)$			0.8			
$\Delta E_R^{pyrite}(MgO_2)$			− 26.8			
$\Delta E_R^{pyrite}(BeO_2)$			− 128.7			

[a] Hartree–Fock (HF), *a posteriori* for electron correlation corrected Hartree–Fock (HF +corr), DFT, and experimental values (kJ/mol) are reported. We calculated from the experimental reaction enthalpies, ΔH_R, reaction energies ΔE_R according to the formula $\Delta E_R = \Delta H_R - p\Delta V_R \approx \Delta H_R - \frac{1}{2}RT = \Delta H_R - 1.2$ kJ/mol (R is the gas constant, T is the experimental reaction temperature: $T = 298.15$ K). The temperature dependencies of ΔE_R are assumed to be negligible. The energies for the peroxides BaO_2, SrO_2, and CaO_2 refer to the calcium carbide structure; additionally we report for CaO_2, MgO_2, and BeO_2 DFT energy values in the pyrite structure.

the DFT values are too small by about 18 kJ/mol. The HF values disagree with the experimental values, as expected from the inaccurate binding energies obtained with the HF method. We note that the peroxide decomposition energy for the HF + corr calculations on SrO_2 is in excellent agreement with the corresponding DFT quantity, while for BaO_2, the HF + corr reaction energy is larger than the DFT value by 18 kJ/mol, but still in relatively good agreement considering the considerable errors in the HF + corr binding energies. This agreement is due to a similar cancellation of errors in the HF + corr and DFT methods as discussed above: the absolute errors in the peroxides are, in both methods, as we have seen, fortunately close to the sum of the absolute errors in the oxides plus half of that in the oxygen molecule. It is difficult to estimate the accuracy of the reaction energies with respect to the experimental values because of the uncertainties in the measured enthalpies, but nevertheless we assume from the above comparison between calculation and experiment that the maximum error is unlikely to be more than 20 kJ/mol.

The most interesting result is that the decomposition energy for CaO_2 is clearly negative, i.e. CaO_2 is, even at 0 K, thermodynamically unstable with respect to decomposition to CaO and O_2. This result confirms the conclusions from our previous structural considerations and is not changed even if we assume the upper value of ±20 kJ/mol for the uncertainty in our calculated DFT reaction energies.

Turning our attention now to the decomposition energies of CaO_2, MgO_2, and BeO_2 in the pyrite crystal structure, calculated with the DFT method and also reported in Table 7, we note first that CaO_2 in this structure is 25.5 kJ/mol more stable than in the calcium carbide structure. We also note that the relative stabilities of CaO_2 in the calcium carbide and the pyrite structure do not, of course, depend on the calculated binding energy of the oxygen molecule, which is substantially overestimated in the DFT calculations. We conclude therefore that calcium peroxide is more stable in the pyrite structure (or in another energetically even more stable structure) and that the calcium carbide structure published by Kotov *et al.* (7) and Brosset *et al.* (8) is incorrect, at least for pure calcium peroxide without water and/or hydrogen peroxide content. However, pure CaO_2 appears, even in the pyrite structure, to be unstable at room temperature, if we take entropy terms into account (as we discuss below).

For MgO_2, we obtained the expected result that the pure compound is also thermodynamically unstable. Our results suggest that the experimentally reported content of H_2O/H_2O_2 in MgO_2 samples (9, 12) is necessary for the stabilization of the compound. Finally, BeO_2 has a huge negative decomposition energy of −129 kJ/mol, which means that it is completely unstable in the pyrite structure, and in view of the magnitude of this term it is certainly not possible, as in the case of MgO_2, to stabilize the compound with H_2O/H_2O_2. BeO_2 is clearly unstable and will not exist under ambient conditions, a conclusion which is entirely compatible with our analysis of metal–oxygen bond lengths reported earlier.

(*c*) *Estimate of the zero point energies and entropies.* We now address the thermodynamics of the peroxide decomposition reaction in more detail. In the discussion above, we considered only the (internal) reaction energies ΔE_R^0 at 0 K; but to study the temperature dependence of the reaction $MO_2 \rightarrow MO + \frac{1}{2}O_2$, we must take entropy terms into account as well and consider the Gibbs free energies ΔG_R^{298} of the reaction:

$$\begin{aligned}\Delta G_R^{298} &= \Delta H_R^{298} - T\Delta S_R^{298}\\ &= \Delta E_R^0 + \Delta E_{vib}^0 + (E^{298} - E^0)_{MO} - (E^{298} - E^0)_{MO_2}\\ &\quad + \tfrac{1}{2}(H^{298} - H^0)_{O_2} - T\Delta S_R^{298}.\end{aligned} \qquad [1]$$

We introduced here, with negligible error, the approximation $E^{298} - E^0 \approx H^{298} - H^0$ for the oxides and the peroxides. ΔE_R^0 are the *ab initio* reaction energies, ΔE_{vib}^0 are the contributions of the zero point vibrational energies, and $-T\Delta S_R^0$ are the contributions of the entropies to the Gibbs free energies of the peroxide decomposition reaction. $E^{298} - E^0$, $(H^{298} - H^0)$ are the energy (enthalpy) changes consequent upon raising the temperature from 0 to 298.15 K. These terms correspond to the vibrational contributions to the (internal) energies at temperatures above 0 K.

In order to obtain estimates for the entropies, zero point energies and energy changes with the temperature of the oxides and peroxides (in the calcium carbide structure) of barium, strontium, and calcium, we performed atomistic lattice simulations based on interatomic potentials. We calculated, from the phonon frequencies, of an optimized structure, these quantities at 298.15 K. The first step for these calculations was to derive a suitable set of interatomic potentials for the alkaline earth metal peroxides, since there are no potentials published. We derived a consistent set of interatomic potentials for the oxides and peroxides by fitting using an energy hypersurface obtained from previous periodic *ab initio* calculations (5) on the peroxides BaO_2, SrO_2, and CaO_2 using the plane-wave, pseudopotential method available in the code Plane_Wave (53) [the pseudopotential method which was reviewed by Payne *et al.* (54) was used]. For the fitting procedure, we simply used formal charges for all the ions. The general procedure for the determination of interatomic potentials from *ab initio* data was described by Gale *et al.* (55). We report the complete set of atomistic interatomic potentials in Table 8. The minimized crystallographic parameters, calculated using these interatomic potentials, are shown in Table 9: the errors in

TABLE 8

Atomistic Buckingham M–O Potentials, $E = Ae^{-r/\rho} - C/r^6$, for the Peroxides (Calcium Carbide Structure) and Oxides of Barium, Strontium, and Calcium, and the Intramolecular Morse Potentials, $E = D_e((1 - e^{-a(r-r_0)2} - 1)$, Acting within the Peroxide Bonds

	M–O_2^{2-} Buckingham potentials			O_2^{2-}–O_2^{2-} Morse potentials		
M	A (eV)	ρ (Å)	C (eV Å^6)	D_e (eV)	a (Å^{-1})	r_0 (Å)
Ba^{2+}	588.31	0.4030	0.0			
Sr^{2+}	819.08	0.3459	0.0			
Ca^{2+}	247.74	0.3996	0.0			
O_2^{2-} (BaO_2)	22764.3	0.1490	253.59	2.4193	2.0984	1.5211
O_2^{2-} (SrO_2)	22764.3	0.1490	33.057	2.3672	2.0139	1.5563
O_2^{2-} (CaO_2)	22764.3	0.1490	0.0000	3.0835	1.5684	1.5976

	M–O^{2-} Buckingham potentials		
M	A (eV)	ρ (Å)	C (eV Å^6)
Ba^{2+}	1464.41	0.3666	0.0
Sr^{2+}	959.58	0.3680	0.0
Ca^{2+}	672.02	0.3690	0.0
O^{2-}	22764.3	0.1490	0.0019

TABLE 9

Crystallographic Parameters of BaO_2, SrO_2, and CaO_2 in the Calcium Carbide Structure and of the Corresponding Oxides Calculated from Atomistic Lattice Simulations Using the Potential Parameters of Table 8; Experimental Values Are Also Reported (for References see Table 1)

	Atomistic lattice simulations			Experimental values		
MO_2	BaO_2	SrO_2	CaO_2	BaO_2	SrO_2	CaO_2
a_0 [Å]	3.785	3.499	3.276	3.806	3.563	(3.54)
c_0 [Å]	6.802	6.582	6.446	6.837	6.616	(5.92)
d_{O-O} [Å]	1.476	1.480	1.480	1.493	1.483	(1.30)
MO	BaO	SrO	CaO	BaO	SrO	CaO
a_0 [Å]	5.506	5.105	4.754	5.539	5.160	4.811

the calculated lattice constants and peroxide bond lengths are generally smaller than 1% (with the exception of CaO_2 of course).

Next, we consider the results from the atomistic lattice simulations. The entropies, zero point vibrational energies, and energy changes with the temperature of the oxides, the peroxides, and the oxygen molecule at room temperature ($T^* = 298.15$ K) are reported in Table 10, together with the contributions of the reaction entropies ($-T^*\Delta S_R^{298}$), zero point energies (ΔE_{vib}^0) and energy changes [$\Delta(E^{298} - E^0)_R$] to the Gibbs free energies and the Gibbs free energies ΔG_R^{298} for the reaction $MO_2 \rightarrow MO + \frac{1}{2}O_2$ (M = Ba, Sr, Ca). The zero point energy of the oxygen molecule was calculated using the *ab initio* quantum chemistry package DMOL (45), as described earlier; for the entropy and energy change with the temperature we took the experimental values of the oxygen molecule (42). In the same table we report also experimental entropies for the oxides, the energy change with the temperature for CaO (42) and the zero point energies for the oxides estimated by the Debye model. We note, first, that the agreement between experimental and calculated entropies, zero point energies and energy changes is good for CaO and SrO. Although the deviations are considerably larger for BaO, it is probable that ΔS_R^{298}, ΔE_{vib}^0, and $\Delta(E^{298} - E^0)_R$ are not affected heavily by this error, because we are dealing here with differences and the errors for BaO and BaO_2 should be of a similar magnitude. Furthermore, we can see that, in all three reactions, the entropy terms favour the decomposition reaction, mainly because the entropy term of the gaseous oxygen molecule is much larger than that of the solid oxides and peroxides, whose entropies additionally cancel each other at least partially. The average entropy contribution to the Gibbs free energies of the peroxide decomposition reaction at 298.15 K is about 20 kJ/mol. We can, of course, calculate the

TABLE 10A

Calculated Entropies (S^{298}), Zero Point Vibrational Energies (E_{vib}^0), and Energy Changes with Temperature ($E^{298} - E^0$) of the Peroxides, Oxides, and the Oxygen Molecule; Available Experimental Values Are Given in Brackets (See Text for References); The Reference Temperature is $T^* = 298.15$ K

	MO			MO_2		
M	S^{298} [J/mol K]	E_{vib}^0 [kJ/mol]	$E^{298} - E^0$ [kJ/mol]	S^{298}[J/mol K]	E_{vib}^0 [kJ/mol]	$E^{298} - E^0$ [kJ/mol]
Ba	55.93 (72.1)	8.77 (4.34)	8.37	85.36	14.50	12.74
Sr	49.32 (54.4)	9.73 (7.50)	7.79	74.96	16.23	11.81
Ca	40.10 (38.1)	11.46 (11.3)	6.84 (6.75)	88.51	14.65	12.45
O_2 molecule	(205.15)	9.02	(8.680)[a]			

[a] $H^{298} - H^0$ [kJ/mol].

TABLE 10B

Contributions of the Reaction Entropies ($-T^*\Delta S_R^{298}$), Zero Point Energies (ΔE^0_{vib}), and Energy Changes [$\Delta(E^{298} - E^0)_R$] to the Gibbs Free Energies and the Gibbs Free Energies ΔG_R^{298} for the Reaction $MO_2 \rightarrow MO + \frac{1}{2}O_2$ (M = Ba, Sr, Ca) (All in kJ/mol)

	$-T^*\Delta S_R^{298}$	ΔE^0_{vib}	$\Delta(E^{298} - E^0)_R$	ΔG_R^{298}
M				
Ba	− 21.8	− 1.2	± 0.0	35.0
Sr	− 22.9	− 2.0	+ 0.3	16.1
Ca	− 16.1	+ 1.3	− 1.3	− 40.8

decomposition temperatures T^{dec}, for which $\Delta G_R^{298} = 0$. It follows from Eq. [1] by neglecting the energy changes with temperature and assuming that the temperature dependencies of ΔS_R^{298} are negligible:

$$T^{dec} = \frac{\Delta E_R^0 + \Delta E^0_{vib}}{\Delta S_R^{298}} \qquad [2]$$

Using Eq. [2] and the DFT values for ΔE_R^0, we calculate for BaO_2 $T^{dec} = 504$°C (777 K) and for SrO_2 $T^{dec} = 231$°C (504 K). These temperatures are somewhat too small compared with the experimental values for complete disintegration of ca. 780°C for BaO_2 and 400°C for SrO_2 obtained from DTA/TG measurements (13, 56). If we use the HF + corr value for ΔE_R^0 for BaO_2, which is 18.4 kJ/mol larger than the DFT value, then we calculate $T^{dec} = 755$°C (1028 K) and obtain a good agreement with the temperatures from DFT/TG measurements. On the other hand, if we compare our calculated DFT decomposition temperatures with the latest values in the "Handbook of Chemistry and Physics" from 1996 (42), which are T^{dec} (BaO_2) = 450°C and T^{dec} (SrO_2) = 215°C and refer to the onset of the decomposition reaction, then we find that our calculated temperatures are in very good agreement with these experimental values, suggesting that our decomposition temperatures and our calculations of the reaction energies ΔE_R^0 and reaction entropies ΔS_R^{298} are reasonable.

We turn now to the calculated zero point energies, ΔE^0_{vib}, and energy changes with temperature, $\Delta(E^{298} - E^0)_R$, for the peroxide decomposition reaction, which are also reported in Table 10. We can see that their values are relatively small and that they are not therefore significantly important for the energetics of the peroxide decomposition reaction. Finally, we calculated the Gibbs free reaction energies, ΔG_R^{298}, for the peroxide decomposition reaction according to Eq. [1]. The Gibbs free reaction energies for BaO_2 and SrO_2 are positive, confirming their stability at room temperature, while for CaO_2 the decomposition reaction energy is negative (− 40.8 kJ/mol). Pure CaO_2 (without H_2O/H_2O_2 content) is therefore thermodynamically unstable, not only at 0 K, as discussed above, but the instability increases with increasing temperature, because the entropy term becomes larger.

4. CONCLUSIONS

The study has amplified considerably our understanding of the energetics of the alkaline earth metal oxides and peroxides and of the peroxide decomposition reaction. In particular, we emphasize the following aspects of our work.

- The comparison between calculated and experimental binding energies indicates that the DFT method and, within limitations, also the Hartree–Fock method with an *a posteriori* correction for the electron correlation are suitable for a correct description of the peroxide bond, for which the Hartree–Fock method is, however, unsuitable.
- The DFT binding energies show, for the alkaline earth metal oxides and peroxides, an impressive agreement with experimental data.
- The DFT reaction energies of the peroxide decomposition $MO_2 \rightarrow MO + \frac{1}{2}O_2$ show that only BaO_2 and SrO_2 are thermodynamically stable compounds, while CaO_2 (calcium carbide structure), MgO_2, and BeO_2 (pyrite structure) are energetically unstable with reaction energies of −24.7, − 26.8, and − 128.7 kJ/mol, respectively, and are therefore unlikely to exist as pure compounds.
- CaO_2 is by 25.5 kJ/mol more stable in the pyrite structure than in the calcium carbide structure. The calculated values of the lattice constants and bond lengths of CaO_2 in the calcium carbide structure give further support for the instability of CaO_2 in the latter structure; they differ substantially from questionable literature data. We conclude, therefore, that the published calcium carbide structure for CaO_2 is incorrect, at least for the pure compound.
- Our analysis suggests that the reported water and/or hydrogen peroxide content of experimentally prepared MgO_2 samples appears to be necessary for the stabilization of the crystal structure.
- BeO_2 is clearly unstable and will not exist under ambient conditions.
- Atomistic simulations predict a negligible effect of the zero point energies on the decomposition energetics, while the entropy terms favor the decomposition reaction by ca. 20 kJ/mol at 298.15 K.

Overall the study shows the value of *ab initio* calculations in probing the structure and stability of oxide materials of this type.

ACKNOWLEDGMENTS

M.K. thanks the DFG (Deutsche Forschungsgemeinschaft) for the financial support of this work. We thank A. Sokol and F. Corà for their constant interest in this work and for helpful and useful discussions. EPSRC is thanked for the provision of the computer hardware at the Royal Institution.

REFERENCES

1. J. D. Bernal, E. Diatlova, I. A. Kazarnovskii, and S. Reichstein, *Z. Kristallogr. A* **92,** 344 (1935).
2. P. D. VerNooy, *Acta Crystallogr. Sect. C* **49,** 433 (1993).
3. W. Wong-Ng and R. S. Roth, *Physica C* **233,** 97 (1994).
4. K.-J. Range, F. Rau, U. Schießl, and U. Klement, *Z. Anorg. Allg. Chem.* **620,** 879 (1994).
5. M. Königstein, "Experimentelle und theoretische Untersuchungen an binären und ternären nichtstöchiometrischen Sauerstoffverbindungen," Dissertation, Universität Regensburg, 1996.
6. M. Königstein, "Crystal Structures of Nonstoichiometric Barium and Strontium Peroxides: BaO_{2-x} $(1.97 \geq 2 - x \geq 1.72)$ and SrO_{2-x} $(1.98 \geq 2 - x \geq 1.90)$." Submitted to *J. Solid State Chem.* (1998).
7. V. Kotov and S. I. Reichstein, *Zhur. Fiz. Khim.* **15,** 1057 (1941).
8. C. Brosset and N.-G. Vannerberg, *Nature* **177,** 238 (1956).
9. N.-G. Vannerberg, *Arkiv Kemi* **14,** 99 (1959).
10. N.-G. Vannerberg, *Arkiv Kemi* **14,** 119 (1959).
11. N.-G. Vannerberg, *Arkiv Kemi* **10,** 455 (1956).
12. A. A. Rywak, J. M. Burlitch, and T. M. Loehr, *Chem. Mater.* **7,** 2028 (1995).
13. W. Hesse, M. Jansen, and W. Schnick, *Prog. Solid State. Chem.* **19,** 47 (1989).
14. P. P. Budnikov and R. A. Belyaev, *Zhur. Prikl. Khim.* **33,** 1921 (1960).
15. "High-Temperature Technology." IL, Moscow, 1959. [Russian translation]
16. I. I. Vol'nov, S. A. Tokareva, E. I. Latysheva, and V. I. Klimanov, *Izv. Akad. Nauk. SSSR, Ser. Khim.* **10,** 2365 (1967).
17. H. A. Wriedt, *Bull. Alloy Phase Diagrams* **6,** 553 (1985).
18. N.-G. Vannerberg, *Prog. Inorg. Chem.* **4,** 125 (1962).
19. M. Königstein, A. A. Sokol, and C. R. A. Catlow, "*Ab Initio* Study of the Structural and Electronic Properties of the Alkaline Earth Metal Peroxides BaO_2, SrO_2 and CaO_2." Submitted to *J. Phys. Condensed Matter* (1998).
20. M. Königstein and C. R. A. Catlow, "*Ab Initio* Quantum Mechanical Study of the Structure and Stability of Nonstoichiometric Barium and Strontium Peroxide." Submitted to *J. Solid State Chem.* (1998).
21. R. Dovesi, V. R. Saunders, C. Roetti, M. Causà, N. M. Harrison, R. Orlando, and E. Aprà, "CRYSTAL95 User's Manual." University of Torino, Torino, Italy, 1996.
22. J. P. Perdew, "Electronic Structure of Solids" (P. Ziesche and H. Eschrig, Eds.), Akademie Verlag, Berlin, 1991.
23. J. P. Perdew, J. A. Chevary, S. H. Vosko, K. A. Jackson, M. R. Pederson, D. J. Singh, and C. Fiolhais, *Phys. Rev. B* **46,** 6671 (1992).
24. M. Causà and A. Zupan, *Chem. Phys. Lett.* **220,** 145 (1994).
25. M. Causà and A. Zupan, *Int. J. Quantum Chem.: Quantum Chem. Symp.* **28,** 633 (1994).
26. (a) J. P. Perdew and Y. Wang, *Phys. Rev. B* **33,** 8800 (1986); (b) **40,** 3399 (1989); (c) **45,** 13244 (1992).
27. A. Lichanot, M. Chaillet, C. Larrieu, R. Dovesi, and C. Pisani, *Chem. Phys.* **164,** 383 (1992).
28. (a) M. I. McCarthy and N. M. Harrison, *Phys. Rev. B* **49,** 8574 (1994). (b) R. Dovesi, C. Roetti, C. Freyria-Fava, E. Aprà, V. R. Saunders, and N. M. Harrison, *Philos. Trans. R. Soc. London, Ser. A* **341,** 203 (1992).
29. C. Freyria-Fava, F. Dovesi, V. R. Saunders, M. Leslie, and C. Roetti, *J. Phys.: Condens. Matter* **5,** 4793 (1993).
30. A. Zupan, I. Petek, M. Causà, and R. Dovesi, *Phys. Rev. B* **48,** 799 (1993).
31. M. Catti, G. Valerio, R. Dovesi, and M. Causà, *Phys. Rev. B* **49,** 14,179 (1994).
32. C. Pisani, R. Dovesi and C. Roetti, "Hartree–Fock *Ab Initio* Treatment of Crystalline Systems," Lecture Notes in Chemistry, Vol. 48. Springer-Verlag, Heidelberg, 1988.
33. J. D. Gale, *J. Chem. Soc., Faraday Trans.* **93,** 629 (1997).
34. J. D. Gale, "GULP User's Manual." Imperial College, 1997.
35. C. R. A. Catlow and W. C. Mackrodt (Eds.), "Computer Simulation in Solids," Lecture Notes in Physics, Vol. 166. Springer-Verlag, Heidelberg, 1982.
36. M. T. Dove, "Introduction to Lattice Dynamics." Cambridge Univ. Press, Cambridge, 1993.
37. A. Zupan and M. Causà, *Int. J. Quantum Chem.* **56,** 337 (1995).
38. R. Pandey, M. Causà, N. M. Harrison, and M. Seel, *J. Phys.: Condens. Matter* **8,** 3993 (1996).
39. P. E. Sinclair and C. R. A. Catlow, *J. Chem. Soc., Faraday Trans.* **93,** 333 (1997).
40. A. Zupan, K. Burke, M. Ernzerhof, and J. P. Perdew, *J. Chem. Phys.* **106,** 10,184 (1997).
41. N. N. Greenwood and A. Earnshaw, "Chemie der Elemente." VCH, Weinheim, 1988.
42. "Handbook of Chemistry and Physics" (R. C. Weast, Ed.). Chemical Rubber Company, Boca Raton, FL, 1996.
43. E. Gmelin, *Z. Naturforsch. A* **24,** 1794 (1969).
44. C. F. Cline, H. L. Dunegan, and G. W. Henderson, *J. Appl. Phys.* **38,** 1944 (1967).
45. "DMOL 96.0/4.0.0 User Guide," September 1996. Molecular Simulations, San Diego, 1996.
46. B. Delley, *J. Chem. Phys.* **92,** 508 (1990).
47. P. Pierron, *Bull. Soc. Chim.* Fr., Mém. **6,** 235 (1939).
48. J. C. Slater, "Quantum Theory of Molecules and Solids, Vol. 1, Electronic Structure of Molecules." McGraw-Hill, New York, 1963.
49. J. A. Alonso and N. A. Cordero, *Int. J. Quantum Chem.: Quantum Chem. Symp.* **29,** 49 (1995).
50. R. de Forcrand, *Ann. Chim. Phys.* **15,** 433 (1908).
51. A. V. Vedeneev, L. J. Kazarnovskaya, and I. A. Kazarnovskii, *Zhur. Fiz. Khim.* **26,** 1808 (1952).
52. M. J. Tribelhorn and M. E. Brown, *Thermochim. Acta* **255,** 143 (1995).
53. "Plane_Wave 4.0.0 User Guide," September 1996. Molecular Simulations, San Diego, 1996.
54. M. C. Payne, M. P. Teter, D. C. Allan, T. A. Arias, and J. D. Joannopoulos, *Rev. Mod. Phys.* **64,** 1045 (1992).
55. J. D. Gale, C. R. A. Catlow, and W. C. Mackrodt, *Model. Simul. Mater. Sci. Eng.* **1,** 73 (1992).
56. I. I. Vol'nov, "Peroxides, Superoxides and Ozonides of Alkali and Alkaline Earth Metals" (A. W. Petrocelli, Ed.), Plenum Press, New York, 1966.
57. A. R. West, "Solid State Chemistry and its Applications." Wiley, New York, 1989.
58. P. Vinet, J. Ferrante, J. R. Smith, and J. H. Rose, *J. Phys. C* **19,** L467 (1986).
59. P. Vinet, J. H. Rose, J. Ferrante, and J. R. Smith, *J. Phys.: Condens. Matter* **1,** 1941 (1989).
60. Z. P. Chang and E. K. Graham, *J. Phys. Chem. Solids* **38,** 1355 (1977).
61. Z. P. Chang and G. R. Barsch, *J. Geophys. Res.* **74,** 3291 (1969).
62. E. H. Riesenfeld and W. Nottebohm, *Z. Anorg. Allg. Chem.* **89,** 405 (1914).